Fano resonances control and slow light with Bose-Einstein Condensate in a nano cavity

M. Javed Akram,[1, *] Fazal Ghafoor,[2, †] M. Miskeen Khan,[1] and Farhan Saif[1, ‡]

[1]*Department of Physics, Quaid-i-Azam University, 45320 Islamabad, Pakistan.*
[2]*Department of Physics, COMSATS Institute of Information Technology, Islamabad, Pakistan*

In this study, a standing wave in an optical nano cavity with Bose-Einstein Condensate (BEC) constitutes one dimensional optical lattice potential in the presence of finite two bodies atomic interaction. We report that interaction of a BEC with standing field in an optical cavity coherently evolve to exhibit Fano resonances in the output field at probe frequency. The behavior of the reported resonance shows an excellent compatibility with the original formulation of asymmetric resonance as discovered by Ugo Fano. Based on our analytical and numerical results, we find that the Fano resonances and subsequently electromagnetically induced transparency of the probe pulse can be controlled through the intensity of the cavity standing wave field and the strength of the atom-atom interaction in the BEC. In addition, enhancement of the slow light effect by the strength of the atom-atom interaction and its robustness against the condensate fluctuations are realizable using presently available technology.

I. INTRODUCTION

Ugo Fano resonance was discovered as the asymmetric feature of a photoionization cross section in an atom. It is attributed to the destructive interference between the probability amplitudes of direct photoionization, and through the auto-ionizing-state indirect photoionization to the ionizing continuum [1–5]. Since its discovery, the asymmetric Fano resonance has been a characteristic feature of interacting quantum systems, such as quantum dots [6, 7], plasmonic nanoparticles [10], photonic crystals [11, 12], phonon transport [13], Mach-Zhender-Fano interferometry [2, 19], whispering-gallery-modes [14, 15], extreme ultraviolet (XUV) attosecond spectroscopy [16], electromagnetic metamaterials [17] and bio-sensors [8, 9]. Fano resonances are characterized by a steeper dispersion than conventional Lorentzian resonances [2, 10], which make them promising for local refractive index sensing applications [17], to confine light more efficiently [2] and for surface enhanced Raman scattering (SERS) [18]. Besides these applications, Fano resonances have also been used for enhancing the biosensing performance [20, 21], enhanced light transmission [22], slow light [23], and classical analog of electromagnetically induced absorption (EIA) [24]. More recently, Heeg et al. [25] reported the use of Fano resonances for interferometric phase detection and x-ray quantum state tomography which provide new avenues for structure determination and precision metrology [25].

In parallel cavity optomechanics [27, 28] has cemented its place in the present-day photonic technology [29, 30]; and serves as basic building block from quantum state-engineering to the quantum communication networks [31, 32]. Due to the ubiquitous nature of the mechanical motion, such resonators couple with many kinds of quantum devices, that range from atomic systems to the solid-state electronic circuits [33–36]. More recently, a new development has been made in the field of levitated optomechanics [37, 38], in which the mechanical oscillator is supported only by the light field. These platforms offer the possibility of a generation of highly-sensitive sensors, which are able to detect (for example) weak forces, with a precision limited only by quantum uncertainties [38]. Fano resonances [39, 40], optomechanically induced transparency [41] with single [42] and multiple windows [40, 43, 44], superluminal and subluminal effects [45–58] have also been observed in optomechanical systems, where nano dimensions and normal environmental conditions have paved the new avenues towards state-of-the-art potential applications, such as imaging and cloaking, telecommunication, interferometry, quantum-optomechanical memory and classical signal processing applications [59–62].

Merging optomechanics with cold atomic systems [63], for instance, Bose-Einstein condensates [64–76] and degenerate cold atom Fermi gases [77] leads to hybrid optomechanical systems. Transition from Mott insulator state to superfluidity of atoms [78] in an optical lattice coupled to a vibrating mirror has been analyzed, as an example of a strongly interacting quantum system subject to the optomechanical interaction [79]. Recently, a comprehensive strategy for using quantum computers to solve models of strongly correlated electrons, using the Hubbard model as a prototypical example has been reported [80]. More recently, interferometric phase detection controlled by Fano resonances and manipulation of slow light propagation have been reported in the x-ray regime [25, 26]. Owing to the significant importance of Fano resonances and slow light in the control of transmission and scattering properties of electromagnetic waves in nano scale devices, we explain the control of the asymmetric sharp and narrow resonances in optomechanics with BEC. In the present paper: (i) we report the emergence of Fano resonances in the presence of BEC in a nano-cavity, where standing cavity field forms the one-dimensional lattice potential [81]. (ii) Upon tuning the

---

* mjakram@qau.edu.pk
† rishteen@yahoo.com
‡ farhan.saif@fulbrightmail.org

resonances versus a wide range of system parameters, we find that the behavior of the resonance reveals an excellent compatibility with the original formulation of asymmetric resonance as discovered by Ugo Fano [1]. (iii) Moreover, we discuss subluminal behavior of the probe field in the system, and explain its parametric dependence. (iv) Unlike previous schemes, we note that the magnitude of slow light can be enhanced by continuously increasing the atom-atom interaction, as well as it is less affected by the condensate fluctuations. This reflects the advantage of present scheme over earlier schemes [52–57], which may help to realize longer optical storage (memory) applications [82–84].

The rest of the paper is organized as follows: In Sec. II, we present the system and formulate the analytical results to explain the Fano resonances and slow light effect based on standard input-output theory. Section III is devoted to compare obtained analytical results with numerical results, where emergence of the Fano resonances is demonstrated. In Sec. IV, we explain slow light and its enhancement in the probe transmission. Finally in Sec. V, we conclude our work.

II. THE MODEL FORMULATION

We consider an optomechanical system with an elongated cigar-shaped Bose-Einstein condensate (BEC) of N two-level ultracold ^{87}Rb atoms (in the $|F = 1\rangle$ state) with m being mass of single atom and ω_a the transition frequency $|F = 1\rangle \rightarrow |F' = 2\rangle$ of the D_2 line of ^{87}Rb. Optical resonator is composed of fixed mirrors which contain a standing wave with frequency ω_c. Hence, we find one dimensional optical lattice potential along the cavity axis, which is coupled strongly with the BEC (see Fig. 1). The system is coherently driven by a strong pump-field of frequency ω_l and a weak probe-field with frequencies $z\omega_p$, respectively. The optomechanical-Bose-Hubbard (OMBH) Hamiltonian of the system can be written as [81, 87, 88],

$$H_T = \hbar\Delta_c c^\dagger c + E_0 \sum_j b_j^\dagger b_j + J_0(\hbar U_0 c^\dagger c + V_{cl}) \sum_j b_j^\dagger b_j$$
$$+ \frac{U}{2} \sum_j b_j^\dagger b_j^\dagger b_j b_j + i\hbar\Omega_l(c^\dagger - c) + i\hbar\varepsilon_p(e^{-i\delta t}c^\dagger - e^{i\delta t}c)$$

where, the first term represents the free Hamiltonian of the single cavity field mode with the creation (annihilation) operator $c^\dagger$ (c). The second term describes the on-site kinetic energy of the condensate with the creation (annihilation) operators $b_j^\dagger$ (b_j) at the jth site. The third term shows the interaction of the condensate with the cavity field. Here, the parameter $U_0 = \frac{g_0^2}{\Delta_a}$ illustrates the optical lattice barrier height per photon and represents the atomic back-action on the field, g_0 is the atom-field coupling and V_{cl} is the classical potential [81]. The fourth term describes the two-body atom-atom interaction, where U is the effective on-site atom-atom in-
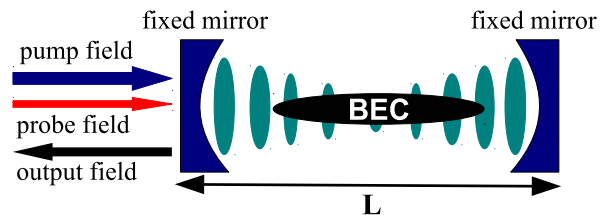

FIG. 1. The schematic representation of the system: an optomechanical system with Bose-Einstein condensate (BEC) confined in an optical cavity with fixed mirrors. A strong driving field of frequency ω_l and a weak probe field of frequency ω_p are simultaneously injected in the cavity.

teraction energy. Finally, the fifth and the sixth terms account for the intense pump laser field and the weak probe laser field, respectively. Here, $\Omega_l = \sqrt{2\kappa P_l/\hbar\omega_l}$ and $\varepsilon_p = \sqrt{2\kappa P_p/\hbar\omega_p}$ are amplitudes of the pump and probe fields, respectively, where P_l (P_p) is the power of the pump (probe) field, and κ is the decay rate of the cavity field. Moreover, $\Delta_c = \omega_c - \omega_l$ and $\delta = \omega_p - \omega_l$ are the respective detuning of the cavity field and the probe field, with pump field frequency ω_l, respectively. Moreover,

$$E_0 = \int d^3x w(\vec{r} - \vec{r}_j)(\frac{-\hbar\nabla^2}{2m})w(\vec{r} - \vec{r}_j),$$
$$J_0 = \int d^3x w(\vec{r} - \vec{r}_j)\cos^2(kx)w(\vec{r} - \vec{r}_j),$$
$$U = \frac{4\pi a_s \hbar^2}{m} \int d^3x w|\vec{r}|^4. \qquad (1)$$

Here in Eq. (1), E_0 and J_0 describes the effective on-site energies of the condensate, defined in terms of the condensate atomic Wannier functions $w(\vec{r} - \vec{r}_j)$, where k is the wave vector, and a_s is the two-body s-wave scattering length [81]. For a detailed analysis of the system, we include photon losses in the system and decay rate associated with the condensate mode, κ and γ_b, respectively. Since here we are interested in the mean response of the coupled system to the probe field in the presence of the pump field, we find the expectation values of operators c and X respectively, where $X = \frac{(b+b^\dagger)}{\sqrt{2}}$ [55]. Based on the Heisenberg equation of motion and the commutation relations $[c, c^\dagger] = 1$ and $[b, b^\dagger] = 1$, the temporal evolutions of $\langle c \rangle$ and $\langle X \rangle$ with the mean-field approximation can be written as [42],

$$\frac{d\langle c \rangle}{dt} = -(\kappa + i\Delta)\langle c \rangle - i\sqrt{2}g\langle X \rangle\langle c \rangle + \Omega_l + \varepsilon_p e^{-i\delta t},$$
$$\langle \ddot{X} \rangle + \gamma_b \langle \dot{X} \rangle + \omega_b^2 \langle X \rangle = -2g(\nu + U_{eff})\langle c^\dagger \rangle\langle c \rangle \qquad (2)$$

where $\Delta = \Delta_c - U_0 N J_0$ is the effective detuning of the cavity field, $g = U_0 J_0 \sqrt{N}|c_s|^2$, $\omega_b = \sqrt{(\nu + U_{eff})(\nu + 3U_{eff})}$, $U_{eff} = \frac{UN}{\hbar M}$, $\nu = U_0 J_0 |c_s|^2 + \frac{V_{cl} J_0}{\hbar} + \frac{E_0}{\hbar}$, and N represents the total number of atoms in M sites. In order to study Fano resonances and slow light, here we are interested in the mean response of the coupled system to the probe field in the presence of the pump field, we do not include quantum fluctuations

which are averaged to zero [42, 53]. This is similar to what has been treated in the context of EIT where one uses atomic mean value equations, and all quantum fluctuations due to both spontaneous emission and collisions are neglected [40, 42]. In order to obtain the steady-state solutions of the above equations, we make the ansatz [89]:

$$\langle c \rangle = c_s + c_- e^{-i\delta t} + c_+ e^{i\delta t},$$
$$\langle X \rangle = X_s + X_- e^{-i\delta t} + X_+ e^{i\delta t}, \tag{3}$$

where c_s and X_s represents the steady-state solutions when $\varepsilon_p = 0$. Moreover, $c_\pm$ and $X_\pm$ are much smaller than c_s and X_s respectively, and are of the same order as ε_p. By substituting Eq. (3) into Eqs. (2), respectively, and taking the lowest order in ε_p but all orders in Ω_l, we get

$$c_s = \frac{\Omega_l}{\kappa + i\Delta}, \tag{4}$$

$$c_- = \frac{[\kappa + i(\Delta - \delta)](\delta^2 - i\delta\gamma_b - \omega_b^2) + ig(\nu + U_{eff})}{[\kappa^2 + \Delta^2 - \delta(\delta + i\kappa)][\delta^2 - i\delta\gamma_b - \omega_b^2] + 2\Delta g(\nu + U_{eff})} \tag{5}$$

In order to study the optical properties of the output field, we use the standard input-output relation viz. [41], $c_{out}(t) = c_{in}(t) - \sqrt{2\kappa}c(t)$. Here, c_{in} and c_{out} are the input and output operators, respectively. We can now obtain the expectation value of the output field as,

$$\langle c_{out}(t) \rangle = (\Omega_l - \sqrt{2\kappa}c_s) + (\varepsilon_p - \sqrt{2\kappa}c_-)e^{-i\delta t} - \sqrt{2\kappa}c_+ e^{i\delta t}. \tag{6}$$

Note that, in analogy with Eq. (3), the second term (on right-hand-side) in the above expression corresponds to the output field at probe frequency ω_p via the detuning $\delta = \omega_p - \omega_l$. Hence, the real and imaginary parts of the amplitude of this term accounts for absorption and dispersion of the whole system to the probe field. Moreover, the transmission of the probe field, which is the ratio of the returned probe field from the coupling system divided by the sent probe field [52], can be obtained as

$$t_p(\omega_p) = \frac{\varepsilon_p - \sqrt{2\kappa}c_-}{\varepsilon_p} = 1 - \frac{\sqrt{2\kappa}c_-}{\varepsilon_p}. \tag{7}$$

For an optomechanical system, in the region of the narrow transparency window, the propagation dynamics of a probe pulse sent to the coupled system greatly alters due to the variation of the complex phase picked up by its different frequency components. The rapid phase dispersion, that is, $\phi_t(\omega_p) = arg[t_p(\omega_p)]$, can cause the transmission group delay given by [28, 52]:

$$\tau_g = \frac{d\phi_t(\omega_p)}{d\omega_p} = \frac{d\{arg[t_p(\omega_p)]\}}{d\omega_p}. \tag{8}$$
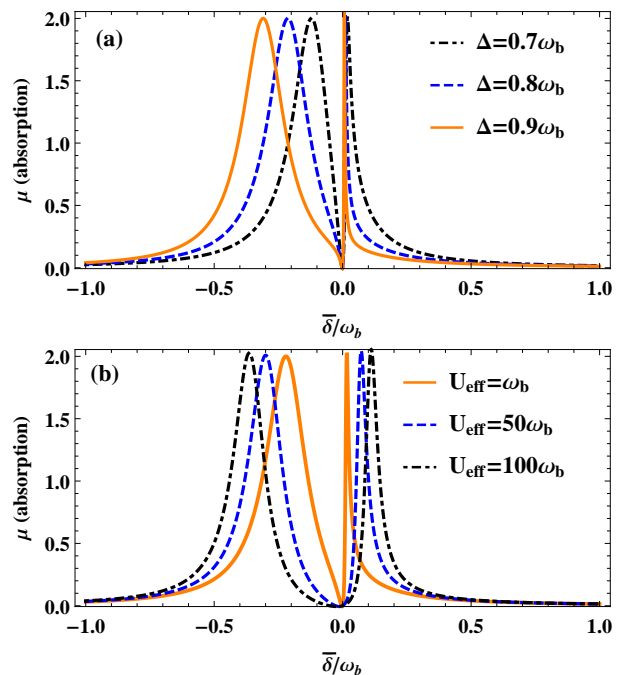

FIG. 2. Fano resonances in the absorption profiles are shown for (a) $\Delta/\omega_b = 0.7, 0.8, 0.9$ corresponding to dot-dashed, dashed and solid curves respectively, and (b) $U_{eff}/\omega_b = 1, 50, 100$, solid, dashed and dot-dashed curves respectively. The rest of the parameters are [66, 71, 72]: $g = 3\omega_b$, $\kappa = 0.1\omega_b$, $U_{eff} = \omega_b$, $\gamma_b/2\pi = 7.5 \times 10^{-3}$ Hz, $\nu/2\pi = 1000$ KHz, $\omega_b/2\pi = 10$ KHz.

III. FANO RESONANCES IN THE OUTPUT FIELD

In this section, the phenomenon of the asymmetric Fano resonances is explained. We note that in absence of the cavity standing wave field, the probe light pulse is absorbed by the condensate attributed to the resonance in frequency of the probe with the Bogoliubov (mechanical) frequency of BEC. On the other hand, quantum interference exhibits in the probe pulse transmission when the oscillation of the cavity standing wave gets in coherence with that of the BEC. Even in the presence of cavity field fluctuation and that of the condensate with finite atomic two-body interaction, the Fano resonance is pronounced.

We observe the resonances in the output field at the probe frequency viz. $E_{out} = \mu + i\nu$. Here, the real and imaginary parts, μ and ν respectively, account for the inphase and out of phase quadratures of the output field at probe frequency corresponding to the absorption and dispersion. Since EIT results from the interference of different frequency contributions, it is well known that we can expect Fano profiles in EIT under certain conditions [4, 14, 39, 40]. For the resonance region $\delta \sim \omega_b$, we analytically obtain the following Fano relation [3],

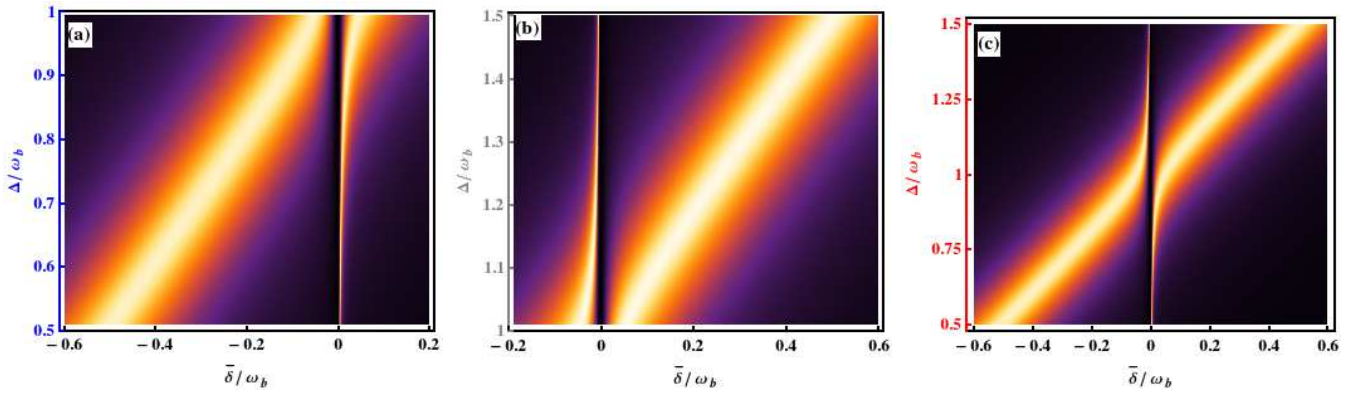$$\mu \approx \frac{2}{1+q^2} \frac{(x+q)^2}{1+x^2}. \tag{9}$$

FIG. 3. Spectrum of Fano resonances in the absorption profiles are shown for a range of specific detuning: (a) For $\Delta/\omega_b = 0.5-1$ i.e. $\Delta < \omega_b$, containing the profiles as shown in Fig. 2(a). (b) For $\Delta/\omega_b = 1.0-1.5$, which shows that narrow and broad regions in Fano profiles can be flipped by suitably tuning the detuning at other side (i.e. $\Delta > \omega_b$) of the resonance $\Delta \sim \omega_b$. (c) For $\Delta/\omega_b = 0.5 - 1.5$, which reflects that Fano spectrum is symmetric around $\Delta \sim \omega_b$. All the other parameters are the same as in Fig. 2

where $x = \frac{\nu+U_{eff}-\omega_b}{\Gamma} - q$, $\Gamma = \frac{2\kappa\Delta g}{\kappa^2+\Omega^2}$, $q = -\Omega/\kappa$, and $\Omega = \Delta - \omega_b$. Interestingly, the absorption profile in Eq. (9) has the same form as the original Fano formula [1, 2] with minimum (zero) and maximum at $x = -q$ and $x = 1/q$, respectively. Here, the asymmetry parameter q is related to the frequency offset Ω which controls the emergence of the asymmetric Fano profiles. Physically it means that the anti-Stokes process is not resonant with the cavity frequency [4, 40].

We first discuss the emergence of Fano resonances in the absorption profile with respect to the effective detuning Δ. We examine Eqs. (5) and (9), when the coupling laser is detuned from the transition $\Delta \leftrightarrow \omega_b$. We present the absorption profiles as a function of normalized detuning $\overline{\delta}/\omega_b$ ($\overline{\delta} = \delta - \omega_b$) in Fig. 2. We note that when detuning of the cavity field Δ is out of resonance with the effective mechanical frequency of the Bogoliubov mode, for instance $\Delta < \omega_b$, consequently Fano shapes appear in EIT spectra [4, 14]. On increasing the detuning Δ, the resonance around $\overline{\delta} \sim \omega_b$ broadens as shown in Fig. 2(a), and all the asymmetric line shapes have a zero at $x = -q$. We note that the interference effects are especially pronounced for small values of q, i.e. when the maximum and minimum are close to each other. In Fig. 2(b), we examine the effect of finite two-body atom-atom interaction on the Fano profiles. Note that, the narrow Fano profile shown as solid line, goes to the relatively broad resonance as we continuously increase the atom-atom interaction U_{eff}, in the vicinity of $\overline{\delta} \sim \omega_b$. The profiles shown in Fig. 2(a) and 2(b) have common minimum or zero, thus these profiles are Fano resonances [3, 4]. It is worthnoting that, as compared to the double-cavity [39] and hybrid atom-cavity [40] optomechanical systems, the Fano resonances in the present model can be controlled by adjusting the atom-atom interaction, and the fluctuations associated with BEC (explained below).

In order to highlight the salient features of Fano resonances, we present the Fano spectra for a range of spe-
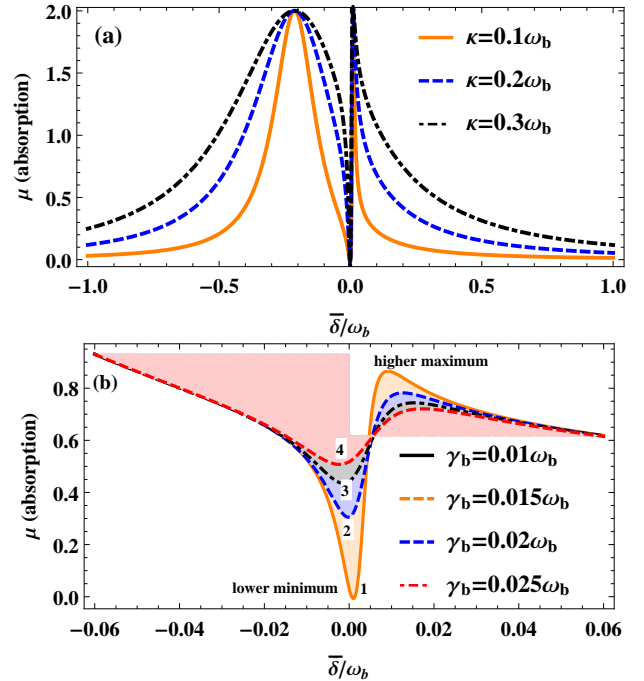

FIG. 4. Fano resonances in the absorption profiles are shown for different values of (a) cavity decay κ, and (b) condensate (Bogoliubov mode) fluctuations γ_b. In (b), we show BEC-cavity setup can pave the way to observe original Fano-like resonances [2] with a lower minimum and a higher maximum. All the other parameters are same as in Fig. 2.

cific detuning as density plots in Fig. 3(a-c) around both sides of the resonance $\Delta \sim \omega_b$. The Fano profiles obtained in Fig. 2(a) (for $\Delta < \omega_b$) belongs to the Fano spectrum as shown in Fig. 3(a). On the other hand, for $\Delta > \omega_b$ while approaching the crossing region [7], we note that the narrow and broad regions in the Fano profiles can be flipped showing the interchange in symmetry

around $\Delta \sim \omega_b$ as shown in Fig. 3(b). Fig. 3(c) encapsulates the Fano spectrum for both sides of the resonance $\Delta \sim \omega_b$, i.e. $\Delta/\omega_b \in [0.5, 1.5]$. It is clear from this figure, which also contains the Fano profiles determined from the corresponding panel of Fig. 2(a), that the two different sets of Fano spectrum in Fig. 3(a) and 3(b) connect smoothly to each other. Most notably, the combination of the two spectra allows the full structure of the anti-crossing between broad and narrow regions to become clear, in agreement with previous reports [7, 12].

The existence of Fano line shapes in BEC-OMS can be understood by noting that the response of the Bogoliubov mode (BEC) features the narrow spectral width, whereas the cavity modes have orders of magnitude higher spectral width and therefore, act as continuum channels [3]. As discussed earlier, the interference of a narrow bound state with a continuum is known to give rise to asymmetric Fano resonances [1–3]. It is worth noting that EIT occurs when the system meet the resonance condition, that is, $\Delta = \omega_b$. However, due to the present non-resonant interactions the symmetry of the EIT window is transformed into asymmetric Fano shapes. Moreover, for optomechanical systems in general, we have two coherent processes leading to the building up of the cavity field: (i) the direct building up due to the application of strong pump and weak probe field, and (ii) the building up due to the two successive nonlinear frequency conversion processes between optical mode and a mechanical mode [28, 39]. These two paths contribute in the interference which leads to the emergence of Fano profiles in the probe absorption spectrum. Hence, broad and narrow regions can be controlled by appropriately adjusting the system parameters in a nano cavity containing BEC.

Furthermore, we note that the cavity decay rate κ and the decay rate of the Bogoliubov mode γ_b plays a vital role in the emergence and control of the Fano resonances. In Fig. 4(a), we indicate that the Fano resonances are sensitive to the cavity decay rate κ. On increasing κ, the resonance around $\bar{\delta} \sim \omega_b$ becomes narrow. These narrow profiles are of primary significance in precision spectroscopy, metrology and high efficiency x-ray detection [25].

At this point, we emphasize that the Fano profiles as explained above, have a fixed (common) minimum. Nevertheless, in Fig. 4(b), we show the magnified Fano resonances for different values of the decay rate of the Bogoliubov mode γ_b, which remarkably yields different minimum points as pointed out by the numbers $1 - 4$. Thus, we observe a higher maximum, and correspondingly, a lower minimum in the Fano profiles as shown in Fig. 4(b). This effect is analogous to the result in the context of photoionization, in which the value of the minimum depends on the radiative effects [1, 2]. Hence, our model not only allows the flexible coherent control to tune the Fano profiles with additional parametric choice (namely the atom-atom interaction) unlike previous schemes [14, 39, 40], but also paves the way towards the observation of original Fano profiles in a single experimental setup with promis-

ing applications, for example, in x-ray detection [25] and ultra-sensitive sensing for biofluid diagnostics [9].

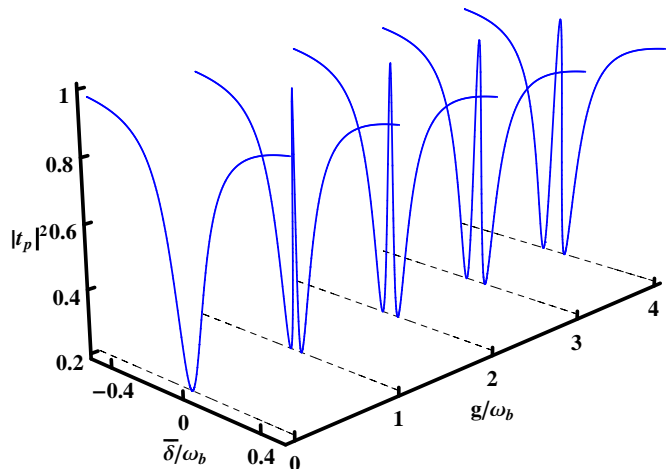## IV. SLOW LIGHT IN THE PROBE TRANSMISSION

FIG. 5. The transmission $|t_p|^2$ of the probe field as functions of normalized probe detuning $\bar{\delta}/\omega_b$ for $\Delta = \omega_b$ and $g/\omega_b = 0, 1, 2, 3, 4$ respectively. All the other parameters are the same as in Fig. 2.

In this section, we analyze the probe field transmission in BEC-cavity setup by utilizing the Bose-Hubbard model. Since both the mirrors are fixed, the interaction between the optical mode and the Bogoliubov mode is analogous to the case of single ended cavity [52] which yields normal dispersion in probe phase, that allows the slow light propagation in the probe transmission. In Fig. 5, we show the transmission $|t_p|^2$ of the probe field as a function of normalized probe detuning ($\bar{\delta}/\omega_b$), versus the normalized coupling strength g/ω_b. We observe that usual Lorentzian curve appears in the transmission spectrum for $g = 0$ at $\bar{\delta} = 0$ ($\bar{\delta} = \omega_b$) in Fig. 5. However, the transparency window [41, 42, 52, 90, 91] occurs in the probe transmission, once the coupling between the cavity field and the condensate mode is present. Figure. 5 depicts that the transparency window in the transmission spectrum broadens and becomes more prominent by continuously increasing the effective coupling strength g. Importantly, unlike traditional optomechanical systems, in addition to the pump laser or the coupling strength, width of the transparency window can effectively be controlled by the atom-atom interaction in our model, as explained in the previous section.

In Fig. 6, we plot the phase of the probe field versus the normalized probe detuning for $\Delta = \omega_b$. Due to coupling of the cavity field with BEC, the phase of the probe field undergoes a sharp enhancement in the resonant region $\bar{\delta} \sim \omega_b$, yielding the rapid phase dispersion [52, 53]. This
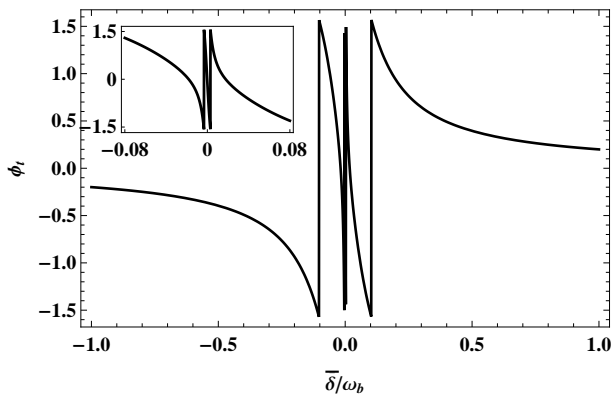
FIG. 6. We plot the phase ϕ_t of the probe field as functions of normalized probe detuning $\overline{\delta}/\omega_b$ for $g = \omega_b$. The inset shows the rapid change around resonance $\overline{\delta} \sim \omega_b$. All the other parameters are the same as in Fig. 5.
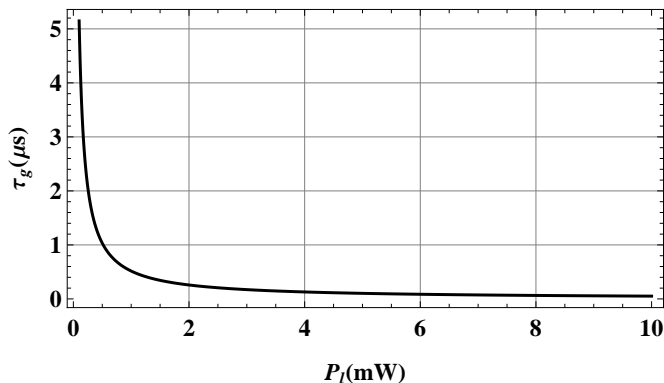

FIG. 7. The group delay τ_g versus the pump power P_l is presented, which shows the pulse delay (subluminal behavior) of the order 5 μs in the probe transmission. All the other parameters are the same as in Fig. 5.

rapid phase dispersion [52, 53] indicates that group delay of the probe field can be changed significantly through the BEC cavity setup. In Fig. 7, we show group delay τ_g versus the pump power P_l. Since the group delay is positive, which reveals that the characteristics of the transmitted probe field exhibits the slow light effect [52, 53, 61, 89].

The slow light propagation in the presence of coupling between the optical mode and condensate mode is analogous to the slow light propagation as reported for the mirror-field coupling in standard optomechanical cavity setups [52, 54, 57]. However, in the former section, we noted that Fano resonances in the probe absorption spectrum are significantly altered by tuning the atom-atom interaction and also affected by the condensate fluctuations. In order to quantify the effect of atom-atom interaction U_{eff} and the fluctuations of the condensate mode γ_b on the probe transmission, we present the group delay τ_g in Fig. 8 and Fig. 9. Interestingly from Fig. 8, we see that on increasing the atomic two-
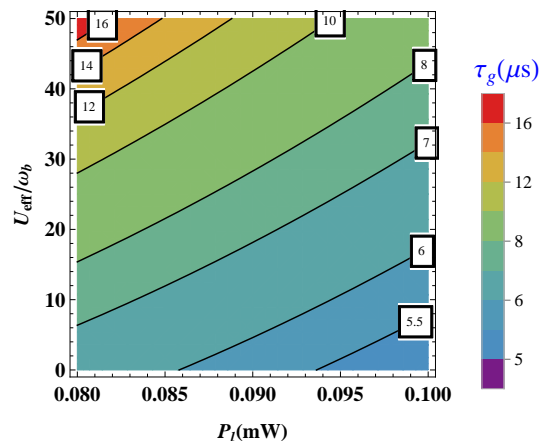

FIG. 8. The group delay τ_g versus the pump power P_l and U_{eff} is presented. The contour plot shows that pulse delay τ_g (subluminal behaviour) can further be enhanced by increasing the atom-atom interaction. All the other parameters are the same as in Fig. 5.

body interaction (U_{eff}), the magnitude of group delay increases. Hence, slow light effect becomes more prominent with large atom-atom interaction, uniquely exist in BEC-cavity setup, and therefore, reflects a clear advantage for the realization of optical memory [82, 83] over previous optomechanics reports on slow light [52–57].

Furthermore, the effect of the condensate fluctuations γ_b on the group delay can be understood from Fig. 9. We note that by tuning γ_b, the group delay remains unaffected or robust (not shown) until condensate fluctuations attains higher values. However, on increasing Γ_b, the magnitude of group delay decreases gradually (where, $\Gamma_b/2\pi = 4.1$ KHz [66] $\approx \omega_b \times \gamma_b$ in magnitude i.e. $\Gamma_b >> \gamma_b$), which indicates that slow light effect in our scheme is capable for optical storage applications [82, 84] owning the great flexibility against the condensate fluctuations. More importantly, unlike single-ended optomechanical systems [52] and hybrid atom-cavity systems [53], the delay-bandwidth product in the present case can be greatly enhanced by continuously increasing atom-atom interaction, and therefore serve as a way to store an optical pulse [82, 84].

Since, such a BEC-cavity setup has also been realized to transfer the quantum state of light fields to the collective density excitations of BEC [88], and plethora of other proposals have been reported to realise an array of connected (coupled) cavities, for example Refs. [85, 86]. We, therefore, anticipate that the present scheme may serve as basic building block to realize quantum networks with longer optical storage [84] leading to the efficient communication between remote cavity setups containing BECs.
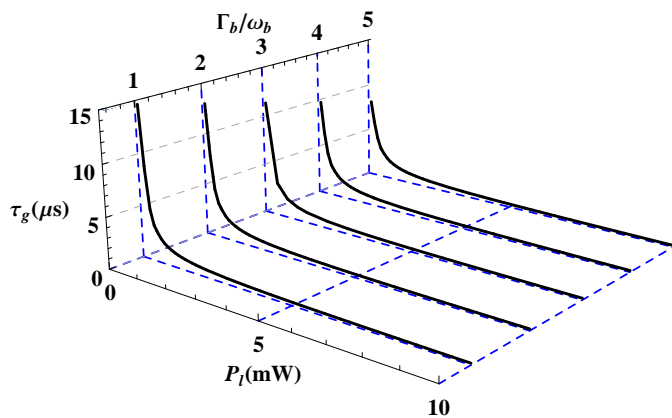
FIG. 9. The group delay τ_g versus the pump power P_l and normalized condensate fluctuations Γ_b/ω_b is presented, which shows that pulse delay (subluminal behaviour) decreases with the increase in the fluctuations of the condensate mode. All the other parameters are the same as in Fig. 5.

V. CONCLUSIONS

In conclusion, we have studied Fano resonances, slow light and its enhancement in a nano cavity containing Bose-Einstein Condensate. It is shown that in the presence of atom-atom interaction, the condensate coherently couples with the cavity standing wave field to exhibit quantum destructive interference. As a result, a typical Fano resonance, which can also be controlled through the strength of atom-atom interaction, is emerged. Moreover, the anti crossing of Fano spectrum and the existence of original Fano profiles in the presence of BEC have been noted. In addition, the occurrence of slow light in the probe transmission is studied, and the group delay is analyzed for the atomic two-body interaction and fluctuations of the condensate. Unlike previous schemes [52–57], by utilizing the Bose-Hubbard model in the present setup, we show that the slow light effect can further be enhanced by increasing the atom-atom interaction.

Despite the promising applications for ultra-sensitive sensing [2, 9, 25] via Fano resonances, it is also safe to predict that interesting applications for optical information storage (memory) and its remote transfer, would be possible by incorporating the extended Bose-Hubbard model [92–95] (to control the group delay with additional interferences by encompassing long-range interactions), as well as to use this technique with coupled cavities [85, 86] containing BECs. Since group delay increases with stronger two-body's atom-atom interaction, the extended BH model together with coupled cavities containing BECs may pave the way for promising and efficient optical information storage applications [82–84], in particular for heralded long-distance quantum communication [96] purposes.

ACKNOWLEDGMENTS

[1] U. Fano, Phys. Rev. **124**, 1866 (1961).

[2] A. E. Miroshnichenko, S. Flach, and Y. S. Kivshar, Rev. Mod. Phys. **82**, 2257 (2010). C. Chin, R. Grimm, P. Julienne, and E. Tiesinga, Rev. Mod. Phys. **82**, 1225 (2010).

[3] C. Ott, A. Kaldun, P. Raith, K. Meyer, M. Laux, J. Evers, C. H. Keitel, C. H. Greene, and T. Pfeifer, Science **340**, 716 (2013).

[4] G. S. Agarwal, *Quantum Optics*, (Cambridge University Press, 2013).

[5] D.-W. Wang, S.-Y. Zhu, J. Evers, and M. O. Scully, Phys. Rev. A **91**, 011801 (2015). W. Chen, K. Zhang, D. S. Goldbaum, M. Bhattacharya, and P. Meystre, Phys. Rev. A **80**, 011801 (2009).

[6] A. C. Johnson, C. M. Marcus, M. P. Hanson, and A. C. Gossard, Phys. Rev. Lett. **93**, 106803 (2004). K. Kobayashi *et al.,* Phys. Rev. B **70**, 035319 (2004). Kuo-Wei Chen, Yu-Hsin Su, Son-Hsien Chen, Chien-Liang Chen, and Ching-Ray Chang, Phys. Rev. B **88**, 035443 (2013). S. Sasaki, H. Tamura, T. Akazaki, and T. Fujisawa Phys. Rev. Lett. **103**, 266806 (2009).

[7] Y. Yoon, M.-G. Kang, T. Morimoto, M. Kida, N. Aoki, J. L. Reno, Y. Ochiai, L. Mourokh, J. Fransson, and J. P. Bird, Phys. Rev. X **2**, 021003 (2012).

[8] A. A. Yanik, A. E. Cetin, M. Huang, A. Artar, S. H. Mousavi, A. Khanikaev, J. H. Connor, G. Shvets, and H. Altug, Proc. Natl. Acad. Sci. U.S.A. **108**, 11784 (2011).

[9] A. Ameen, M. R. Gartia, A. Hsiao, T. W. Chang, Z. D. Xu, and G. L. Liu, J. Nanomater. **2015**, 35 (2015).

[10] B. Luk'yanchuk *et al.*, Nat. Mater. **9**, 707 (2010). S. Xiao *et al.,* Fortschr. Phys. **61**, 348 (2013).

[11] M. V. Rybin, A. B. Khanikaev, M. Inoue, K. B. Samusev, M. J. Steel, G. Yushin, and M. F. Limonov, Phys. Rev. Lett. **103**, 023901 (2009). M. Rahmani *et al.,* Nano Lett. **12**, 2101 (2012). W. Ding, B. Luk'yanchuk, and C. W. Qiu Phys. Rev. A **85**, 025806 (2012). S. Nojima, M. Usuki, M. Yawata, and M. Nakahata Phys. Rev. A **85**, 063818 (2012). Guo Liang Shang, Guang Tao Fei, *et al.,* Sci. Rep. **4**, (2014).

[12] A. Christ, S. G. Tikhodeev, N. A. Gippius, J. Kuhl, and H. Giessen, Phys. Rev. Lett. **91**, 183901 (2003). A. Christ, T. Zentgraf, J. Kuhl, S. G. Tikhodeev, N. A. Gippius, and H. Giessen, Phys. Rev. B **70**, 125113 (2004).

[13] T. T. Tang, Y. Zhang, C. H. Park, B. Geng, C. Girit, Z. Hao, M. C. Martin, A. Zettl, M. F. Crommie, S. G. Louie, Y. R. Shen, and F. Wang, Nat. Nanotechnol. **5**, 32 (2010).

[14] B. Peng, S. K. Özdemir, W. Chen, F. Nori, and L. Yang, Nature Commun. **5**, 5082 (2014).

[15] F. Lei, B. Peng, S. K. Özdemir, G. L. Long, and L. Yang, Appl. Phys. Lett. **105**, 101112 (2014). Y. L. Li, J. Millen, and P. F. Barker, arXiv:1508.06217 [physics.optics] (2015).

[16] C.-T. Liao, A. Sandhu, S. Camp, K. J. Schafer, and M. B. Gaarde, Phys. Rev. Lett. **114**, 143002 (2015). C.-T. Liao, A. Sandhu, S. Camp, K. J. Schafer, and M. B. Gaarde, Phys. Rev. A **93**, 033405 (2016).

[17] N. Verellen *et al.,* Nano Lett. **9**, 1663 (2009). J. Wallauer and M. Walther, Phys. Rev. B **88**, 195118 (2013).

[18] J. Ye *et al.,* Nano Lett. **12**, 1660 (2012).

[19] A. E. Miroshnichenko, and Y. S. Kivshar, Appl. Phys. Lett. 95, 121109 (2009).

[20] N. Verellen *et al.,* Nano Lett. **11**, 391 (2011).

[21] C. Wu *et al.,* Nat. Mater. **11**, 69 (2012).

[22] Z. K. Zhou *et al.*, Nano Lett. **11**, 49 (2011).

[23] S. Zhang, D. A. Genov, Y. Wang, M. Liu and X. Zhang, Phys. Rev. Lett. **101**, 047401 (2008).

[24] R. Taubert, M. Hentschel, J. Kästel and H. Giessen, Nano Lett. **12**, 1367 (2012).

[25] K. P. Heeg, C. Ott, D. Schumacher, H.-C. Wille, R. Röhlsberger, T. Pfeifer, and J. Evers, Phys. Rev. Lett. **114**, 207401 (2015).

[26] K. P. Heeg, J. Haber, D. Schumacher, L. Bocklage, H.-Ch. Wille, K. S. Schulze, R. Loetzsch, I. Uschmann, G. G. Paulus, R. Rüffer, R. Röhlsberger, and J. Evers, Phys. Rev. Lett **114**, 203601 (2015).

[27] P. Meystre, Ann. Phys. (Berlin) **525**, 215 (2013).

[28] M. Aspelmeyer, T. J. Kippenberg, F. Marquardt, Rev. Mod. Phys. **86**, 1391 (2014).

[29] B. Rogers, N. Lo Gullo, G. De Chiara, G. M. Palma, and M. Paternostro, Quantum Meas. Quantum Metrol. **2**, 11 (2014).

[30] G. Kurizki, P. Bertet, Y. Kubo, K. Mølmer, D. Petrosyan, P. Rabl, and J. Schmiedmayer, PNAS **112**, 3866 (2015).

[31] J. I. Cirac, and P. Zoller, Nature (London) **404**, 579 (2000).

[32] T. D. Ladd, F. Jelezko, R. Laflamme, Y. Nakamura, C. Monroe, and J. L. O'Brien, Nature (London) **464**, 45 (2010).

[33] L. Tian, Ann. Phys. (Berlin) **527**, 1 (2015).

[34] L. Tian, and P. Zoller, Phys. Rev. Lett. **93**, 266403 (2004).

[35] W. K. Hensinger et al., Phys. Rev. A **72**, 041405(R) (2005).

[36] M. J. Akram, K. Naseer, and F. Saif, arXiv:1503.01951 [quant-ph] (2015). M. J. Akram and F. Saif, Nonlinear Dyn. **83**, 963-970 (2016).

[37] T. S. Monteiro, J. Millen, G. A. T. Pender, F. Marquardt, D. Chang, and P. F. Barker, New J. Phys **15**, 015001 (2013). G. A. T. Pender, P. F. Barker, F. Marquardt, J. Millen, and T. S. Monteiro, Phys. Rev. A **85**, 021802 (2012).

[38] J. Millen, P. Z. G. Fonseca, T. Mavrogordatos, T. S. Monteiro, and P. F. Barker, Phys. Rev. Lett. **114**, 123602 (2015). P. Z. G. Fonseca, E. B. Aranas, J. Millen, T. S. Monteiro, and P. F. Barker, arXiv:1511.08482 [quant-ph] (2015).

[39] K. Qu and G. S. Agarwal, Phys. Rev. A **87**, 063813 (2013).

[40] M. J. Akram, F. Ghafoor, and F. Saif, J. Phys. B: At. Mol. Opt. Phys. **48**, 065502 (2015).

[41] S. Weis, R. Riviére, S. Deléglise, E. Gavartin, O. Arcizet, A. Schliesser, and T. J. Kippenberg, Science **330**, 1520 (2010).

[42] G. S. Agarwal and S. Huang, Phys. Rev. A **81**, 041803(R) (2010).

[43] H. Wang, X. Gu, Y. X. Liu, A. Miranowicz, and F. Nori, Phys. Rev. A **90**, 023817 (2014).

[44] M. Paternostro, M. S. Kim, and B. S. Ham, Phys. Rev. A **67**, 023811 (2003). F. Ghafoor, Laser Phys. **24**, 035702 (2014). S. Huang and M. Tsang, arXiv:1403.1340 [quant-ph] (2014). M. J. Akram, F. Ghafoor, and F. Saif, arXiv:1512.07297 [quant-ph] (2015).

[45] L. V. Hau, S. E. Harris, Z. Dutton, and C. H. Behroozi, Nature (London) **397**, 594 (1999).

[46] M. M. Kash, V. A. Sautenkov, A. S. Zibrov, L. Hollberg, G. R. Welch, M. D. Lukin, Y. Rostovtsev, E. S. Fry, and M. O. Scully, Phys. Rev. Lett. **82**, 5229 (1999).

[47] Y. Okawachi, M. A. Foster, J. E. Sharping, A. L. Gaeta, Q. Xu, and M. Lipson, Opt. Express **14**, 2317 (2006). S. L. Mouradian, T. Schröder, C. B. Poitras, L. Li, J. Goldstein, E. H. Chen, M. Walsh, J. Cardenas, M. L. Markham, D. J. Twitchen, M. Lipson, and D. Englund, Phys. Rev. X, **5**, 031009 (2015).

[48] B. Macke and B. Ségard, Phys. Rev. A **78**, 013817 (2008). B. Macke and B. Ségard, Opt. Commun. **281**, 12 (2008). Bruno Macke and Bernard Ségard, Phys. Rev. A **82**, 023816 (2010). B. Ségard and B. Macke, Phys. Lett. A **109**, 213 (1985).

[49] G. S. Agarwal, T. N. Dey, and S. Menon, Phys. Rev. A **64**, 053809 (2001). M. Sahrai, H. Tajalli, K. T. Kapale, and M. Suhail Zubairy, ibid. **70**, 023813 (2004).

[50] M. O. Scully and M. S. Zubairy, Science **301**, 181 (2003). R. W. Boyd and D. J. Gauthier, Science 326, 1074 (2009).

[51] M. D. Stenner, D. J. Gathier and M. A. Niefeld, Nature **425**, 695 (2003).

[52] A. H. Safavi-Naeini, T. P. Alegre, J. Chan, M. Eichenfield, M. Winger, Q. Lin, J. T. Hill, D. E. Chang, and O. Painter, Nature (London) **472**, 69 (2011).

[53] M. J. Akram, M. M. Khan, and F. Saif, Phys. Rev. A **92**, 023846 (2015).

[54] D. Tarhan, S. Huang, and O. E. Mustecaplioglu, Phys. Rev. A **87**, 013824 (2013). D. Tarhan, Act. Phys. Pol. A **124**, 46 (2013).

[55] B. Chen, C. Jiang, and K. D. Zhu, Phys. Rev. A **83**, 055803 (2011).

[56] X-G Zhan *et al.,* J. Phys. B: At. Mol. Opt. Phys. **46**, 025501 (2013).

[57] C. Jiang, H. Liu, Y. Cui, X. Li, G. Chen, and B. Chen, Opt. Express **21**, 12165 (2013).

[58] J. Q. Liang, M. Katsuragawa, F. L. Kien, and K. Hakuta, Phys. Rev. A **65**, 031801(R) (2002). F. Le Kien and K. Hakuta, Phys. Rev. A **79**, 013818 (2009).

[59] R. W. Boyd and D. J. Gauthier, Progress in Optics 43, edited by E. Wolf, Chap. 6, p. 497. (Elsevier, Amsterdam, 2002).

[60] D. E. Chang, A. H. Safavi-Naeini, M. Hafezi, and O. Painter, New J. Phys **13**, 023003 (2011).

[61] P. W. Milonni, *Fast light, slow light and lefthanded light* (Institute of Physics Publishing, Bristol, 2005).

[62] F. Ghafoor, B. A. Bacha, and S. Khan, Phys. Rev. A **91**, 053807 (2015). M. M. Khan, M. J. Akram, and F. Saif, arXiv:1511.07617 [quant-ph] (2015).

[63] D. Hunger, S. Camerer, M. Korppi, A. Jöckel, T. W. Hänsch, and P. Treutlein, C. R. Phys. **12**, 871 (2011).

[64] W. Petrich, M. H. Anderson, J. R. Ensher, and E. A. Cornell, Phys. Rev. Lett. **74**, 3352 (1995). K. B. Davis, M. -O. Mewes, M. R. Andrews, N. J. van Druten, D. S. Durfee, D. M. Kurn, and W. Ketterle Phys. Rev. Lett. **75**, 3969 (1995).

[65] S. Martelucci, A. N. Chester, A. Aspect, and M. Inguscio, *Bose-Einstein Condensation and Atom Lasers*, New York: Kluwer academic publisher (2002).

[66] F. Brennecke, S. Ritter, T. Donner, and T. Esslinger, Science **322**, 235 (2008). F. Brennecke, T. Donner, S. Ritter, T. Bourdel, M. Köhl, and T. Esslinger, Nature (London) **450**, 268 (2007).

[67] L. D. Carr, D. DeMille, R. V. Krems, and J. Ye, New J. Phys. **11**, 055049 (2009). L. H. Haddad and L. D. Carr, New J. Phys. **17**, 093037 (2015). L. H. Haddad and L. D. Carr, New J. Phys. **17**, 063034 (2015).

[68] G. De Chiara, M. Paternostro, and G. M. Palma, Phys. Rev. A **83**, 052324 (2011). B. Rogers, M. Paternostro, G. M. Palma, and G. De Chiara, Phys. Rev. A **86**, 042323 (2012).

[69] J. A. Dunningham, S. Bose, L. Henderson, V. Vedral, and K. Burnett, Phys. Rev. A **65**, 064302 (2002). I. Fuentes-Guridi, J. Pachos, S. Bose, V. Vedral, and S. Choi, Phys. Rev. A **66**, 022102 (2002). H. T. Ng and S. Bose, Phys. Rev. A **78**, 023610 (2008).

[70] M. Asjad and F. Saif, Phys. Rev. A **84**, 033606 (2011). M. Asjad and F. Saif, Phys. Lett. A **376**, 2608 (2012).

[71] K. W. Murch et al., Nat. Phys. **4**, 561 (2008).

[72] A. Schliesser et al., Nat. Phys. **4**, 415 (2008).

[73] W. Chen, D. S. Goldbaum, M. Bhattacharya, and P. Meystre, Phys. Rev. A **81**, 053833 (2010).

[74] H. D. Jing, D. S. Goldbaum, L. Buchmann, and P. Meystre, Phys. Rev. Lett. **106**, 223601 (2011).

[75] S. K. Steinke, S. Singh, M. E. Tasgin, P. Meystre, K. C. Schwab, and M. Vengalattore, Phys. Rev. A **84**, 023841 (2011). O. Zobay, G. Metikas, and G. Alber, Phys. Rev. A **69**, 063615 (2004). G. Alber, Phys. Rev. A **63**, 023613 (2001). G. Alber and G. Metikas, Appl. Phys. B: Lasers Opt. **B73**, 773 (2001).

[76] M. Jääskeläinen and P. Meystre, Phys. Rev. A **71**, 043603 (2005). M. Jääskeläinen and P. Meystre **73**, 013602 (2006). M. Jääskeläinen, J. Jeong, and C. P. Search, Phys. Rev. A **76**, 063615 (2007). J. O. Weatherall, C. P. Search, and M. Jääskeläinen, Phys. Rev. A **78**, 013830 (2008).

[77] P. Kanamoto and P. Meystre Phys. Rev. Lett. **104**, 063601 (2010). M. Asjad, M. A. Shahzad, and F. Saif, Eur. Phys. J. D **67**, 198 (2013). S. Yang, M. Al-Amri, and M. S. Zubairy, J. Phys. B: At. Mol. Opt. Phys. **47** 135503 (2014).

[78] C. E. Creffield and T. S. Monteiro, Phys. Rev. Lett. **96**, 210403 (2006).

[79] J. Larson, Damski, G. Morigi, and M. Lewenstein, Phys. Rev. Lett. **100**, 050401 (2008).

[80] D. Wecker, M. B. Hastings, N. Wiebe, B. K. Clark, C. Nayak, and M. Troyer, Phys. Rev. A **92**, 062318 (2015).

[81] O. Morsch and M. Oberthaler, Rev. Mod. Phys. **78**, 179 (2006). I. B. Mekhov, and H. Ritsch, J. Phys. B: At. Mol. Opt. Phys. **45**, 102001 (2012).

[82] C. Simon *et al.*, Eur. Phys. J. D **58**, 1 (2010).

[83] D. D. F. Phillips, A. Fleischhauer, A. Mair, R. L. Walsworth, and M. D. Lukin, Phys. Rev. Lett. **86**, 783 (2001).

[84] P. Jobez, N. Timoney, C. Laplane, J. Etesse, A. Ferrier, P. Goldner, N. Gisin, and M. Afzelius, Phys. Rev. A **93**, 032327 (2016). H. Wu, R. E. George, J. H. Wesenberg, K. Mølmer, D. I. Schuster, R. J. Schoelkopf, K. M. Itoh, A. Ardavan, J. J. L. Morton, and G. A. D. Briggs, Phys. Rev. Lett. **105**, 140503 (2010).

[85] A. S. Parkins and H. J. Kimble, J. Opt. B, Quantum Semiclass. Opt. **1**, 496 (1999). M. Paternostro, W. Son, and M. S. Kim, Phys. Rev. Lett. **92**, 197901 (2004). M. Paternostro, W. Son, M. S. Kim, G. Falci, and G. M. Palm, Phys. Rev. A **70**, 022320 (2004).

[86] A. Xuereb, and P. Domokos, New J. Phys. **14**, 095027 (2012). A. Xuereb, C. Genes, and A. Dantan, Phys. Rev. Lett. **109**, 223601 (2012). A. Xuereb, C. Genes, and A. Dantan, Phys. Rev. A **88**, 053803 (2013).

[87] A. B. Bhattacherjee, Phys. Rev. A **80**, 043607 (2009). A. Bhattacherjee, Opt. Commun. **281**, 3004 (2008).

[88] T. Kumar, A. B. Bhattacherjee, P. Verma, and ManMohan, J. Phys. B: At. Mol. Opt. Phys. **44**, 065302 (2011).

[89] R. W. Boyd, *Nonlinear Optics*, Academic Press, New York, (2010).

[90] S. E. Harris, Phys. Today **50**, 36 (1997). S. E. Harris, J. E. Field, and A. Imamoglu, Phys. Rev. Lett. **64**, 1107 (1990). K. J. Boller, A. Imamoglu, and S. E. Harris, Phys. Rev. Lett. **66**, 2593 (1991). M. O. Scully, and M. S. Zubairy, Quantum Optics, Cambridge: Cambridge University Press (1997).

[91] M. Fleischhauer, A. Imamoglu, and J. P. Marangos, Rev. Mod. Phys. **77**, 633 (2005).

[92] S. Baier, M. J. Mark, D. Petter, K. Aikawa, L. Chomaz, Z. Cai, M. Baranov, P. Zoller, and F. Ferlaino, arXiv:1507.03500 [cond-mat.quant-gas] (2015).

[93] D. Rossini and R. Fazio, New J. Phys. **14**, 065012 (2012).

[94] J. Miao, Phys. Rev. A **92**, 023632 (2015).

[95] G. Corrielli, A. Crespi, G. Della Valle, S. Longhi, and R. Osellame, Nat. Commun. **4**, 1555 (2013).

[96] H. J. Kimble, Nature (London) **453**, 1023 (2008).